

Direct Interactions with Three-Particle Final States

M. M. DUNCAN AND J. L. DUGGAN
University of Georgia, Athens, Georgia

AND

R. D. PURRINGTON
A & M College of Texas, College Station, Texas
(Received 1 November 1963)

Momentum and angular distributions have been calculated for a reaction of the type $\text{Li}^7(\text{He}^3, n\text{p})\text{Be}^8$ using a plane-wave stripping-type interaction. These calculations are compared to the neutron time-of-flight data for this reaction which have been measured at an incident He^3 energy of 2 MeV.

INTRODUCTION

THE neutron time-of-flight data for the bombardment of Li^7 by He^3 shows a continuous distribution of neutron energies. It has been shown that this continuum exists for all neutron energies below those associated with the reaction $\text{Li}^7(\text{He}^3, n)\text{B}^9$ and above the detection limit associated with the plastic scintillator detector.¹⁻³ A previous theoretical treatment of reactions of the type $(\text{He}^3, n\text{p})$, based on a different approximation has been given by Demeur.⁴ The calculations presented here are based on a plane-wave stripping-type interaction with cutoff and including recoil effects so that one can hope for only qualitative agreement with the experimental data. The calculations show that even though one is dealing with a three-body final state, there are characteristic shapes to the angular distributions for a fixed value of the observed momentum. Also, the treatment given here neglects the effects of spin since these can be included by inspection of the work of Demeur.⁴

THE CROSS SECTION

The notation is as follows: The subscripts 1, 2, and C refer to the three nucleons of He^3 . Nucleons 1 and 2 are the free final-state nucleons and C is captured by the target A to form the final nucleus B . Only particle 1 is detected. Neutron and proton masses are assumed equal. The differential cross section for measuring particle 1 within a solid angle $d\Omega_1$, and with momentum between $\hbar\mathbf{k}_1$ and $\hbar(\mathbf{k}_1 + d\mathbf{k}_1)$ is

$$\left(\frac{d\sigma}{d\Omega_1 dk_1}\right) d\Omega_1 dk_1 = \frac{2\pi}{\hbar I} \sum_f |M|^2 \frac{d\mathbf{k}_1}{(2\pi)^3} \frac{k_2^2 d\Omega_2 dk_2}{(2\pi)^3 dE}. \quad (1)$$

The sum is over all the final states of the particles which are consistent with energy and momentum conservation. I is the incident flux, and M is the matrix element.

¹ J. L. Duggan, M. M. Duncan, P. D. Miller, and R. F. Gabbard, *Bull. Am. Phys. Soc.* **7**, 59 (1962).

² J. L. Duggan, P. D. Miller, and R. F. Gabbard, *Nucl. Phys.* **46**, 336 (1963).

³ M. M. Duncan, J. L. Duggan, and R. D. Purrington, *Bull. Am. Phys. Soc.* **8**, 114 (1963).

⁴ M. Demeur, *Physica* **20**, 1189 (1954).

Now,

$$E = \frac{\hbar^2 k_1^2}{2m} + \frac{\hbar^2 k_2^2}{2m} + \frac{\hbar^2 (\mathbf{k}_1 + \mathbf{k}_2)^2}{2m_B} \quad (2)$$

is the total energy in the center-of-mass system. (All quantities are in the center-of-mass system unless otherwise stated.) m is a nucleon mass and m_B is the final nuclear mass. For fixed \mathbf{k}_1 Eq. (2) gives

$$\frac{dk_2}{dE} = \hbar^{-2} \left[\left(\frac{1}{m} + \frac{1}{m_B} \right) k_2 + \frac{\mathbf{k}_1 \cdot \mathbf{k}_2}{m_B k_2} \right]^{-1}, \quad (3)$$

and according to (2) k_2 is a function of direction for a fixed \mathbf{k}_1 , thus,

$$\frac{d\sigma}{d\Omega_1 dk_1} = [\hbar I (2\pi)^5]^{-1} k_1^2 \int d\Omega_2 k_2^2 \frac{dk_2}{dE} |M|^2. \quad (4)$$

The matrix element M can be calculated from the method given by Tobocman.⁵ One obtains

$$M = \int d\mathbf{R}_1 d\mathbf{R}_2 d\mathbf{R}_c d\xi \exp[-i(\mathbf{k}_1 \cdot \mathbf{R}_1 + \mathbf{k}_2 \cdot \mathbf{R}_2 + \mathbf{k}_B \cdot \mathbf{R}_B)] \\ \times \psi_B^*(\xi, \mathbf{r}_c) (\sum V) \exp[i(\mathbf{k}_3 \cdot \mathbf{R}_3 + \mathbf{k}_A \cdot \mathbf{R}_A)] \\ \times \psi_A(\xi) \psi_3(\mathbf{R}_1, \mathbf{R}_2, \mathbf{R}_c).$$

Here

$$\sum V = V_{1c} + V_{2c} + V_{12} + V_{1A} + V_{2A}$$

are the interaction potentials, the \mathbf{R}_i refers to the position of the i th particle in the center-of-mass system, and the \mathbf{k}_i are the momenta of the particles, with $(\mathbf{k}_3, \mathbf{R}_3)$ referring to the incident He^3 .

Conservation of linear momentum and the definitions

$$\mathbf{p}_1 = \mathbf{R}_1 - \mathbf{R}_c, \quad \mathbf{p}_2 = \mathbf{R}_2 - \mathbf{R}_c, \quad \mathbf{r}_c = \mathbf{R}_c - \mathbf{R}_A, \\ \mathbf{K}_1 = \mathbf{k}_1 - \mathbf{k}_3/3, \quad \mathbf{K}_2 = \mathbf{k}_2 - \mathbf{k}_3/3,$$

and

$$\mathbf{K}_c = \mathbf{k}_3 - (m_A/m_B)(\mathbf{k}_1 + \mathbf{k}_2)$$

⁵ W. Tobocman, *Phys. Rev.* **94**, 1655 (1954).

allow one to write the matrix element as

$$M = \int d\boldsymbol{\rho}_1 d\boldsymbol{\rho}_2 d\mathbf{r}_c d\xi \exp[-i(\mathbf{K}_1 \cdot \boldsymbol{\rho}_1 + \mathbf{K}_2 \cdot \boldsymbol{\rho}_2)] \\ \times \psi_3(\rho_1, \rho_2, |\boldsymbol{\rho}_1 - \boldsymbol{\rho}_2|) \\ \times (\sum V) \psi_B^*(\xi, \mathbf{r}_c) \psi_A(\xi) \exp[i\mathbf{K}_c \cdot \mathbf{r}_c].$$

Now one makes the usual simple stripping approximations, that is, particles 1 and 2 are not to penetrate the surface of A , $V_{1A} + V_{2A}$ are not effective, and the integration over \mathbf{r}_c is restricted to values of $r_c \geq R$. Furthermore, it is assumed that

$$\psi_B^*(\xi, \mathbf{r}_c) = \psi_A^*(\xi) \psi_i^*(r_c).$$

The potentials $V_{12} + V_{1c} + V_{2c}$, can be removed by a standard mathematical operation.⁶ Consider the internal He^3 Hamiltonian,

$$H = T_1 + T_2 + T_c + V_{12} + V_{1c} + V_{2c} \\ = -(\hbar^2/2m)(\nabla_{\rho_1}^2 + \nabla_{\rho_2}^2 + \text{grad}_{\rho_1} \cdot \text{grad}_{\rho_2}) \\ + V_{12} + V_{1c} + V_{2c}.$$

Then

$$\sum V = H - T_1 - T_2 - T_3,$$

and the matrix element M can be expressed as

$$M = T(\mathbf{K}_1, \mathbf{K}_2) \int d\boldsymbol{\rho}_1 d\boldsymbol{\rho}_2 \exp[-i(\mathbf{K}_1 \cdot \boldsymbol{\rho}_1 + \mathbf{K}_2 \cdot \boldsymbol{\rho}_2)] \psi_3 \\ \times \int_{r_c \geq R} d\mathbf{r}_c \psi_i^*(r_c) \exp[i\mathbf{K}_c \cdot \mathbf{R}_c],$$

$$T(\mathbf{K}_1, \mathbf{K}_2) = -[\epsilon_3 + \hbar^2/2m(K_1^2 + K_2^2 + \mathbf{K}_1 \cdot \mathbf{K}_2)],$$

where ϵ_3 is the binding energy of the He^3 .

If one now uses the He^3 wave function given by Bruno,⁷

$$\psi_3 = N_3 \exp[-\gamma^2(\rho_1^2 + \rho_2^2 + |\boldsymbol{\rho}_1 - \boldsymbol{\rho}_2|^2)],$$

and evaluates the last integral as in ordinary stripping, ($l \neq 0$),

$$M = N_3 T(\mathbf{K}_1, \mathbf{K}_2) \left(\frac{2\pi}{\sqrt{3}\gamma^2} \right)^{3/2} \\ \times \exp[-(K_1^2 + K_2^2 + \mathbf{K}_1 \cdot \mathbf{K}_2)/6\gamma^2] \\ \times i^l [4\pi(2l+1)]^{1/2} [h_l^{(1)}(i\beta R)] \\ \times [(K_c R) j_{l-1}(K_c R) - \Lambda_l j_l(K_c R)] R / (\beta^2 + K_c^2).$$

Here

$$\Lambda_l = l+1 + \beta R \frac{d}{d(\beta R)} \ln h_l^{(1)}(i\beta R),$$

⁶ M. Banerjee, in *Nuclear Spectroscopy*, edited by F. Ajzenberg-Selove (Academic Press Inc., New York, 1960).

⁷ B. Bruno, *Arkiv. Mat. Astron. Fys.* A36, No. 8 (1948).

and

$$\beta = \left(\frac{2mm_A}{m+m_A} \frac{\epsilon_{CB}}{\hbar^2} \right)^{1/2}.$$

ϵ_{CB} is the separation energy of C from B . From conservation of energy,

$$\frac{T(\mathbf{K}_1, \mathbf{K}_2)}{\beta^2 + K_c^2} = \frac{m+m_A}{mm_A} \hbar^2$$

and therefore one can collect all constants and use (4) to obtain

$$\frac{d\sigma}{d\Omega_1 d\mathbf{k}_1} = N k_1^2 \int d\Omega_2 k_2^2 \frac{dk_2}{dE} \\ \times \exp[-(K_1^2 + K_2^2 + \mathbf{K}_1 \cdot \mathbf{K}_2)/3\gamma^2] \\ \times |(K_c R) j_{l-1}(K_c R) - \Lambda_l j_l(K_c R)|^2.$$

RESULTS

This cross section, Eq. (5), has been calculated for various values of R and l for the fixed value of γ^2 suggested by Bruno.⁷ (Trial calculations indicated that the results are not a strong function of the value of γ .) The results of the calculations are given in Figs. 1, 2, and 3. Note that these calculations have been made for the reaction $\text{Li}^7(\text{He}^3, n\text{p})\text{Be}^8$ for the case where Be^8 is in its ground state and the case where Be^8 is in its first excited state. However, from angular momentum and parity considerations one expects only the $l=1$ calculation to be valid for this reaction. The other l values are calculated merely to indicate the shapes of the distributions. Also, the width of the first excited state of Be^8 has not been introduced as we believe that this will not qualitatively change the results.

Figures 4 and 5 show the comparison of the calculations with the experimental data. The experimental

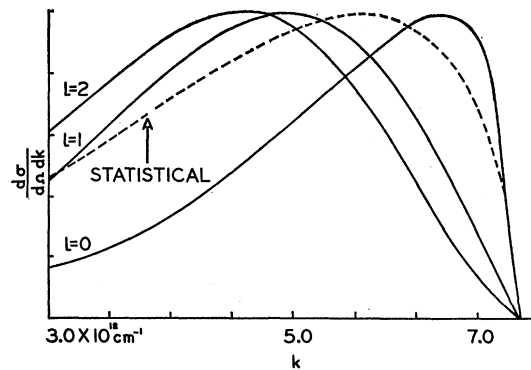


Fig. 1. Calculated momentum distributions at $\theta_c = 0^\circ$ for various values of the captured orbital angular momentum assuming Be^8 is formed in the ground state. $E(\text{He}^3) = 2$ MeV, and $R = 3 \times 10^{-13}$ cm. The purely statistical distribution is shown as a dashed curve.

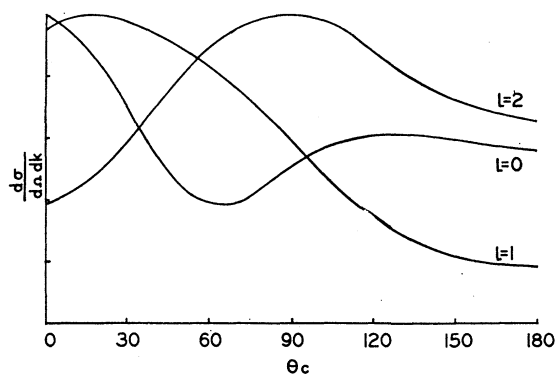


FIG. 2. Calculated angular distributions for a fixed momentum of the captured particle ($k=5 \times 10^{12} \text{ cm}^{-1}$) assuming Be^8 is in the ground state. $E(\text{He}^3)=2 \text{ MeV}$, and $R=3 \times 10^{-13} \text{ cm}$.

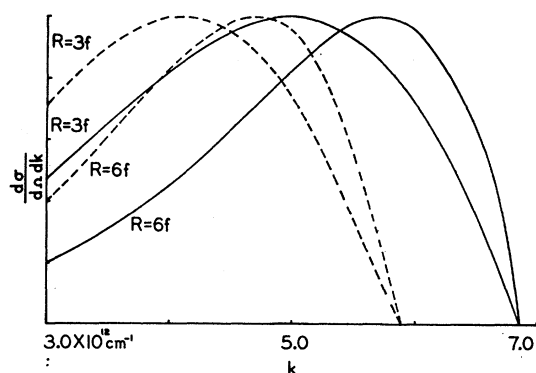


FIG. 3. A comparison of the calculated momentum spectra at $\theta_c=0^\circ$, $E(\text{He}^3)=2 \text{ MeV}$, $l=1$, for two different values of R . The solid curves assume Be^8 in the ground state and the dashed curves assume Be^8 in the first excited state.

techniques and the neutron time-of-flight system that were used for these measurements have been discussed elsewhere.² In Fig. 4 the experimental data is drawn as a smooth curve and the errors shown are representative statistical ones. Only part of the neutron spectrum is shown. At higher neutron momenta one sees the neutron groups from the reaction $\text{Li}^7(\text{He}^3, n)\text{B}^9$. At low-neutron energies the uncertainty in the efficiency of the plastic scintillator detector gives a large uncertainty in determining the differential cross section. Therefore the lower momentum experimental data is not shown.

In both Figs. 4 and 5 the theoretical curves are based on the assumption that the reaction proceeds via the first excited state of Be^8 . The only justification for this is that the momentum distributions associated with the ground-state reaction do not give good agreement. All three angular distribution curves of Fig. 5 have the same normalization.

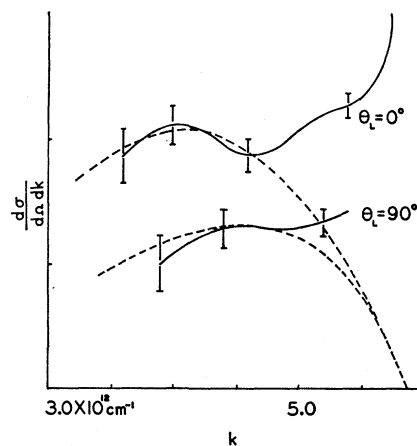


FIG. 4. A comparison of the experimental data at 2 MeV and the calculated momentum spectra for two laboratory angles assuming $l=1$, $R=3 \times 10^{-13} \text{ cm}$, and Be^8 in its first excited state. The smooth solid curve is the average experimental data.

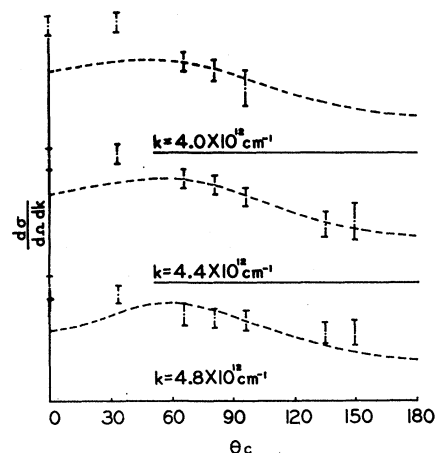


FIG. 5. A comparison of the experimental angular distributions at 2 MeV for three different momentum values. $R=3 \times 10^{-13} \text{ cm}$, $l=1$, and Be^8 is assumed to be in the first excited state.

It is clear that the agreement is not overwhelming, but one should not expect quantitative fits from this type of calculation. On the other hand, it is felt that these results are encouraging enough to warrant further investigation, both experimentally and theoretically, and these will be presented in the future.

ACKNOWLEDGMENT

We would like to thank William Meggs for help with some of the preliminary calculations and the computing facilities of both the University of Georgia and the A & M College of Texas.